ISSN 0020-1685, *Inorganic Materials*, 2006, Vol. 42, No. 10, pp. 1121–1125. © Pleiades Publishing, Inc., 2006.
Original Russian Text © O.Z. Yanchevskii, A.G. Belous, A.I. Tovstolytkin, O.I. V'yunov, D.A. Durilin, 2006, published in Neorganicheskie Materialy, 2006, Vol. 42, No. 10, pp. 1229–1233.

Structural, Electrical, and Magnetic Properties of $La_{0.7}Sr_{0.3}Mn_{1-y}Cr_yO_3$

O. Z. Yanchevskii[a], A. G. Belous[a], A. I. Tovstolytkin[b], O. I. V'yunov[a], and D. A. Durilin[a]
[a] *Vernadsky Institute of General and Inorganic Chemistry, National Academy of Sciences of Ukraine,*
pr. Akademika Palladina 32/34, Kiev, 03680 Ukraine
[b] *Institute of Magnetism, National Academy of Sciences of Ukraine,*
bul'v. Akademika Vernadskogo 36b, Kiev, 03142 Ukraine
e-mail: yanch@ionc.kar.net

Received December 27, 2004; in final form, April 24, 2006

Abstract—Detailed structural data are presented for $La_{0.7}Sr_{0.3}Mn_{1-y}Cr_yO_3$ solid solutions with $0 < y \le 0.10$. Chromium substitution on the manganese site is shown to reduce the T_C of the solid solutions at a rate of 4 K/mol % Cr. The 300-K magnetoresistance of $La_{0.7}Sr_{0.3}Mn_{1-y}Cr_yO_3$ attains 8% in a field of 1.2 MA/m.

DOI: 10.1134/S002016850610013X

INTRODUCTION

In the last decade, there has been considerable interest in $Ln_{1-x}M_xMnO_3$ (Ln = La, Nd, Pr; M = Ca, Sr, Ba, Pb) substituted manganites, motivated by their colossal magnetoresistance (MR) [1–3].

To date, most research effort has been concentrated on the effect of Ln-site substitutions on the MR and T_C of manganites. At the same time, substitutions of 3*d* transition metals for manganese on the B site may also influence the $Mn^{3+} : Mn^{4+}$ ratio, give rise to local lattice strain, and, eventually, alter the electrical and magnetic properties of the material. In this context, Cr substitution appears interesting. The Cr^{3+} ion is identical in electronic configuration to Mn^{4+} and is Jahn–Teller inactive. It is well known that $Cr^{3+}–O^{2-}–Mn^{4+}$ magnetic interaction is favorable for ferromagnetic ordering [4, 5].

Most studies concerned with the effect of chromium doping have been concentrated on the $Ln_{0.5}M_{0.5}MnO_3$ (Ln = La, Nd, Pr, Sm; M = Ca, Sr) manganites [6–10], in which chromium induces a transition from anti- to ferromagnetic ordering below room temperature. At the same time, there is considerable scientific and practical interest in the study of $La_{0.7}Sr_{0.3}Mn_{1-y}Cr_yO_3$ materials with $T_C \ge 300$ K, which exhibit the strongest magnetoresistive response near room temperature [11].

In this paper, we report the structural, magnetic, electrical, and magnetoresistive properties of $La_{0.7}Sr_{0.3}Mn_{1-y}Cr_yO_3$ (LSMCr) solid solutions with $0 < y \le 0.10$.

EXPERIMENTAL

LSMCr samples (y = 0, 0.02, 0.04, 0.06, 0.08, 0.10, 0.12) for this investigation were prepared by solid-state reactions, using appropriate mixtures of predried extra-pure-grade La_2O_3 and Mn_2O_3 and reagent-grade Cr_2O_3 and $SrCO_3$. The starting mixtures were homogenized by milling for 8 h in bidistilled water with corundum grinding media. Next, the mixtures were dried, screened through a nylon-6 sieve, and fired at 1220 and 1240 K for a total of 4 h with intermediate grindings. After addition of a binder, the powder was pressed into disks 10–15 mm in diameter and 3–4 mm in thickness, which were then sintered at 1570–1670 K for 2 h.

The Mn^{3+} and Mn^{4+} contents of the samples were determined by titrating iodine with a sodium thiosulfate solution. Iodine in a potassium iodide solution was replaced by chlorine resulting from the dissolution of a manganite sample in hydrochloric acid.

X-ray diffraction (XRD) measurements were performed on a DRON 4-07 powder diffractometer (CuK_α radiation). The structural parameters of polycrystalline samples were refined by the Rietveld profile analysis method.

Ferromagnetic resonance (FMR) spectra were recorded on a RADIOPAN spectrometer, using rectangular samples 1 × 1 × 5 mm in dimensions. The applied magnetic field was parallel to the long axis of the sample.

The electrical resistivity ρ of ceramic samples was measured by a four-probe technique from 77 to 370 K. The samples were rectangular in shape, 2 × 3 × 10 mm in dimensions. Electrical contacts were made by firing silver paste. Magnetoresistance $(\rho_0 - \rho_H)/\rho_0 \times 100\%$, where ρ_0 is the zero-field resistivity and ρ_H is the resis-

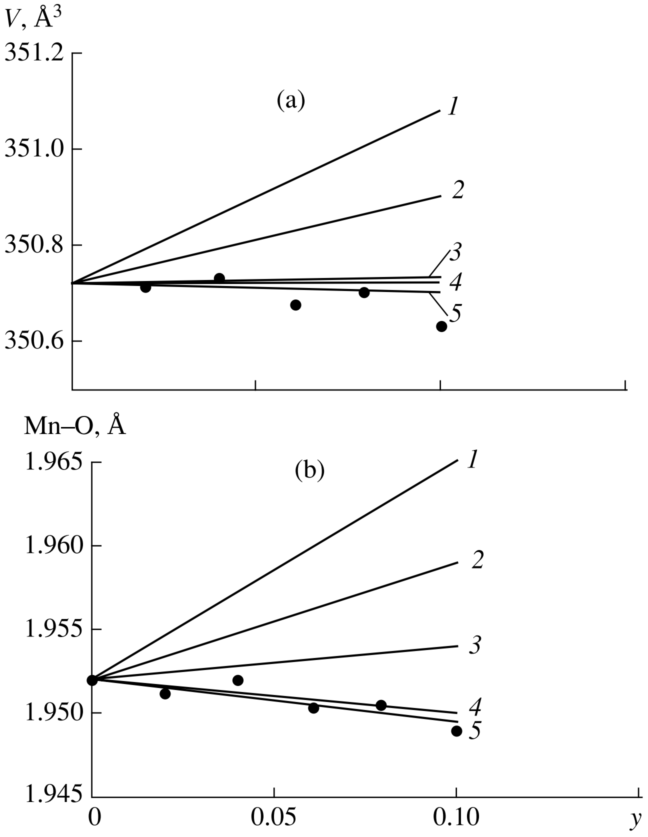

Fig. 1. (a) Unit-cell volume and (b) Mn–O bond distance as functions of chromium content for $La_{0.7}Sr_{0.3}Mn_{1-y}Cr_yO_3$ solid solutions: experimental data (points) in comparison with calculation results in different charge compensation models (solid lines): (*1*) $3Mn^{4+} \longrightarrow 2Mn^{3+} + Cr^{6+}$, (*2*) $2Mn^{4+} \longrightarrow Mn^{3+} + Cr^{5+}$, (*3*) $Mn^{4+} \longrightarrow Cr^{4+}$, (*4*) $2Mn^{3+} \longrightarrow Mn^{4+} + Cr^{2+}$, (*5*) $Mn^{3+} \longrightarrow Cr^{3+}$.

tivity in magnetic field *H*, was determined in applied fields of up to 1.2 MA/m.

RESULTS AND DISCUSSION

XRD examination showed that all of the synthesized LSMCr materials ($0 \le y \le 0.1$) were single-phase and had a rhombohedral structure (sp. gr. $R\bar{3}c$). The structural parameters of the LSMCr samples are listed in the table.

Figure 1 shows the experimentally determined unit-cell volume and Mn–O bond distance in LSMCr as functions of chromium content in comparison with those calculated in different models for charge compensation in chromium-doped manganites. As the input data, we used the experimental results obtained earlier for $La_{0.7}Sr_{0.3}MnO_3$ [12]. For each plausible charge compensation mechanism, we calculated the relative changes in unit-cell volume and bond distances as functions of chromium content, using Shannon's system of ionic radii [13]. In our calculations, manganese was taken to be present only in the oxidation states 3+ and 4+ [14], whereas the oxidation state of chromium was free to vary from 2+ to 6+ [15]. As seen in Fig. 1, the data points fall close to lines *4* and *5*, which represent the following charge compensation mechanisms:

$$2Mn^{3+} \longrightarrow Mn^{4+} + Cr^{2+}, \qquad (I)$$

$$Mn^{3+} \longrightarrow Cr^{3+}. \qquad (II)$$

To find out which mechanism, *I* or *II*, underlies charge compensation in LSMCr, we analyzed magnetic data. Figure 2 shows the fraction of manganese ions in the oxidation state 4+, Mn^{4+}/Mn, calculated as a function of *y* for mechanisms *I* and *II*. First, we assumed that Cr is not involved in double exchange (lines *I*, *II*). The fraction of Mn^{4+} was evaluated from chemical analysis data for $y = 0$ and using the model schemes (*I*) and (*II*) for $x > 0$. Sr-doped manganites are known [16, 17] to contain a ferromagnetic phase if the Mn^{4+}/Mn ratio lies in the range 0.18 to 0.50 (dashed region in Fig. 2). Beyond this range, there is a tendency toward antiferromagnetic ordering, which results in antiferromagnetism or a more complex magnetic structure [16, 17]. It follows from Fig. 2 that, for $y \ge 0.03$, the magnetic phase is likely to decompose into two phases (lines *I*, *II*). However, according to Ghosh et al. [18] and Gross et al. [19], LSMCr solid solutions remain ferromagnetic over the entire composition range studied here ($0 \le y \le 0.10$).

Crystal data for $La_{0.7}Sr_{0.3}Mn_{1-y}Cr_yO_3$ solid solutions sintered at 1670 K

y	0	0.02	0.04	0.06	0.08	0.10
a, Å	5.5125(3)	5.5121(5)	5.5120(5)	5.5118(2)	5.5117(2)	5.5115(5)
c, Å	13.3304(4)	13.3303(3)	13.3305(7)	13.3284(3)	13.3289(3)	13.3287(7)
V, Å^3	350.80(3)	350.75(2)	350.74(5)	350.66(2)	350.66(2)	350.64(5)
$z_{O(1)}$	0.460(4)	0.463(4)	0.465(6)	0.468(5)	0.456(3)	0.461(6)
χ^2	1.231	1.194	1.235	1.164	1.128	1.195
R_B, %	5.67	6.71	8.55	8.48	6.59	6.15
R_f, %	5.97	7.50	8.13	8.00	6.44	6.30
Mn–O, Å	1.9520	1.9515	1.9521	1.9506	1.9508	1.9495

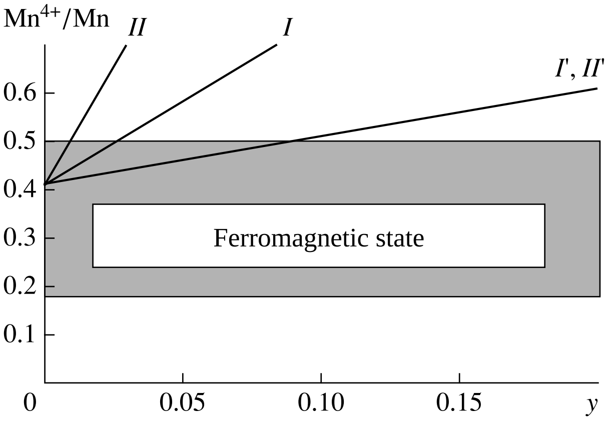

Fig. 2. Composition dependences of Mn^{4+}/Mn in $La_{0.7}Sr_{0.3}Mn_{1-y}Cr_yO_3$ calculated for the charge compensation mechanisms (*I*, *I'*) $2Mn^{3+} \longrightarrow Mn^{4+} + Cr^{2+}$ and (*II*, *II'*) $Mn^{3+} \longrightarrow Cr^{3+}$; (*I*, *II*) Cr is assumed not to be involved in double exchange, (*I'*, *II'*) Cr participates in double exchange.

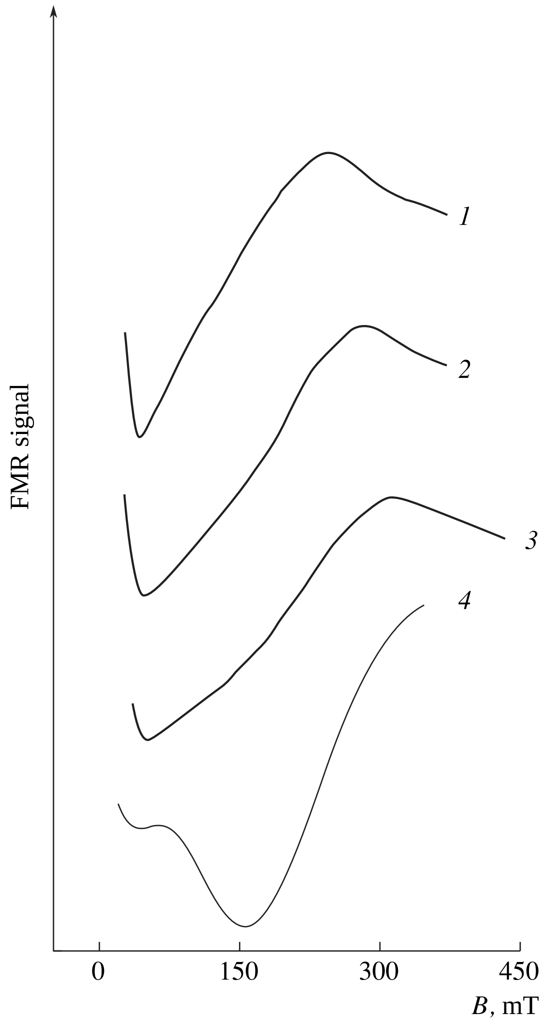

Fig. 3. 77-K FMR spectra of $La_{0.7}Sr_{0.3}Mn_{1-y}Cr_yO_3$ samples with y = (*1*) 0, (*2*) 0.04, (*3*) 0.08, and (*4*) 0.12.

This is supported by the fact that the shape of their FMR spectra varies only slightly with composition (Fig. 3). Thus, we are led to conclude that Cr participates in double exchange. Then, given that Mn^{4+} and Cr^{3+} have identical electronic configurations ($3d^3$), as do Mn^{3+} and Cr^{2+} ($3d^4$), we obtain identical composition dependences of the fraction of $3d^3$ ions (Fig. 2, lines *I'*, *II'*). Therefore, magnetic data provide no way of discriminating between mechanisms *I* and *II*. At the same time, the FMR spectrum of the $y = 0.12$ sample shows a peak at $B = 20$ mT (Fig. 3, spectrum *4*), which can be interpreted as evidence that this sample is magnetically inhomogeneous, in accordance with the proposed charge compensation model.

According to earlier results [20], the MR of single-crystal manganites has a maximum near T_C. The temperature dependences of MR and normalized resistivity in Fig. 4 indicate that chromium substitution for manganese in LSMCr shifts the peak in ρ_n to lower temperatures compared to the peak in MR. The difference in

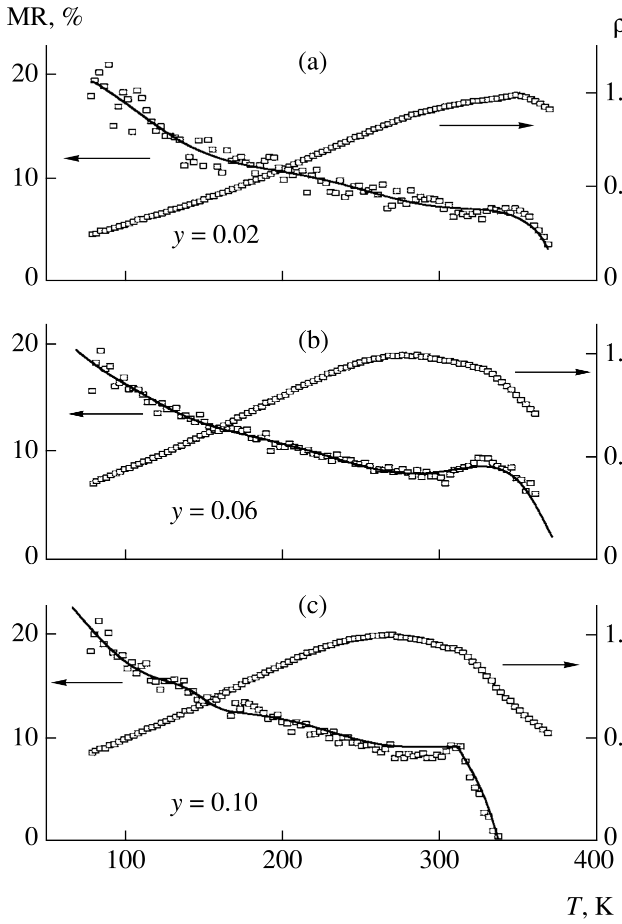

Fig. 4. Temperature dependences of normalized resistivity $\rho_n = \rho_i/\rho_{max}$ and magnetoresistance for polycrystalline $La_{0.7}Sr_{0.3}Mn_{1-y}Cr_yO_3$ with y = 0.02, 0.06, and 0.10.

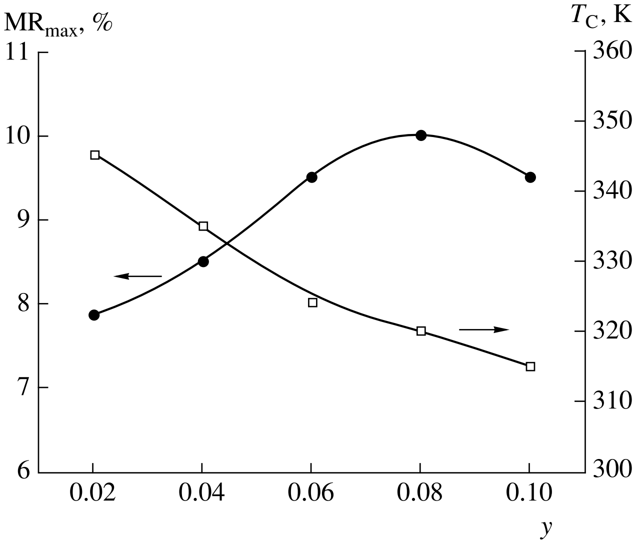

Fig. 5. Effect of chromium doping on the maximum MR (H = 1.2 MA/m) and T_C of $La_{0.7}Sr_{0.3}Mn_{1-y}Cr_yO_3$ ceramics.

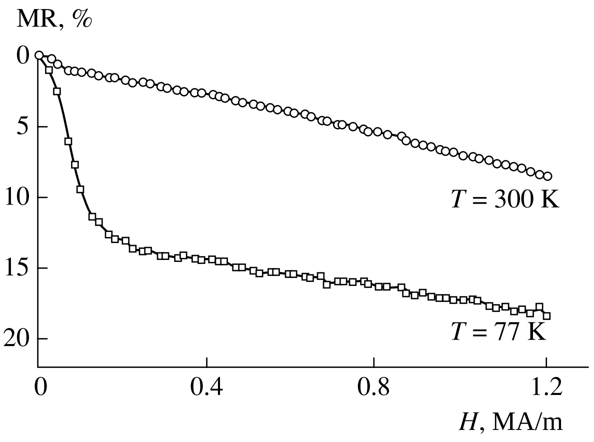

Fig. 6. Effect of magnetic field on the MR of $La_{0.7}Sr_{0.3}Mn_{0.9}Cr_{0.1}O_3$ ceramic at 300 and 77 K.

the peak ρ_n and peak MR temperatures may be due to local structural distortions resulting from chromium substitution on the manganese site. At low temperatures ($T < T_C$), the MR of polycrystalline LSMCr rises steadily with decreasing temperature. This behavior of MR may be due to spin-dependent scattering of charge carriers in intergranular regions [21] or spin-polarized tunneling through grain boundaries [18].

Figure 5 illustrates the effect of chromium doping on the maximum MR (H = 1.2 MA/m) and Curie temperature of $La_{0.7}Sr_{0.3}Mn_{1-y}Cr_yO_3$. Over the entire composition range studied ($0 \le y \le 0.10$), MR_{max} varies only slightly, within the range 8–10%. Chromium substitution on the manganese site reduces T_C at a rate of 4 K/mol % Cr.

The effect of magnetic field on the MR of the $La_{0.7}Sr_{0.3}Mn_{0.9}Cr_{0.1}O_3$ ceramic at 77 and 300 K is illustrated in Fig. 6. Note that the 300-K MR is a linear function of magnetic field, which is crucial for the practical application of such materials.

CONCLUSIONS

We determined the structure and composition of $La_{0.7}Sr_{0.3}Mn_{1-y}Cr_yO_3$ solid solutions in the range $0 < y \le 0.12$. Comparing model calculation results and experimental data, we confirmed the presence of Cr^{3+} in these materials. Chromium substitution on the manganese site reduces their T_C at a rate of 4 K/mol % Cr. The 300-K MR of $La_{0.7}Sr_{0.3}Mn_{1-y}Cr_yO_3$ is a linear function of magnetic field and attains 8% in a field of 1.2 MA/m.

REFERENCES

1. Cherepanov, V.A., Barkhatova, L.Yu., and Voronin, V.V., Phase Equilibria in the La–Sr–Mn–O System, *J. Solid State Chem.*, 1997, vol. 134, no. 1, pp. 38–44.
2. Kamata, H., Yonemura, Y., Mizusaki, J., et al., High Temperature Electrical Properties of the Perovskite-Type Oxide $La_{1-x}Sr_xMnO_{3-\delta}$, *J. Phys. Chem. Solids*, 1995, vol. 56, no. 7, pp. 943–950.
3. Tokura, Y., Uruschibara, A., Maritomo, Y., et al., Giant Magnetotransport Phenomena in Filling-Controlled Kondo Lattice System: $La_{1-x}Sr_xMnO_3$, *J. Phys. Chem. Soc. Jpn*, 1994, vol. 63, no. 11, pp. 3931–3935.
4. Martin, C., Maignan, A., Hervieu, M., et al., Influence of Mn-Site Doping upon Orbital and Charge Ordering in the $Pr_{0.5}A_{0.5}Mn_{1-x}M_xO_3$, *J. Magn. Magn. Mater.*, 1999, vol. 202, pp. 11–21.
5. Zhang, L.W., Gong Feng, Liang He, et al., The Magnetotransport Properties of $LaMn_{1-x}Cr_xO_3$, *J. Magn. Magn. Mater.*, 2000, vol. 219, pp. 236–240.
6. Raveau, B., Maignan, A., and Martin, C., Insulator–Metal Transition Induced by Cr and Co Doping in $Pr_{0.5}Ca_{0.5}MnO_3$, *J. Solid State Chem.*, 1997, vol. 130, p. 162–166.
7. Bernabe, A., Maignan, A., Hervieu, M., et al., Extension of Colossal Magnetoresistance Properties to Small A-Site Cations by Chromium Doping in $La_{0.5}Ca_{0.5}MnO_3$, *Appl. Phys. Lett.*, 1997, vol. 71, no. 26, pp. 3907–3909.
8. Mahendiran, R., Hervieu, M., Maignan, A., et al., Coexistence of Ferromagnetism and Charge Ordering in $Pr_{0.5}Ca_{0.5}Mn_{1-x}Cr_xO_3$, *Solid State Commun.*, 2000, vol. 114, pp. 429–433.
9. Schuddinck, W., Van Tendello, G., Bernabe, A., et al., Relation between Structure, Charge Ordering, and Magnetotransport Properties in $Nd_{0.5}Ca_{0.5}Mn_{1-x}Cr_xO_3$ Manganites, *J. Magn. Magn. Mater.*, 2000, vol. 211, pp. 105–110.
10. Kallel, N., Dhahri, J., Zemni, S., et al., Effect of Cr-Doping in $La_{0.7}Sr_{0.3}Mn_{1-x}Cr_xO_3$ $0 \le x \le 0.5$, *Phys. Status Solidi*, 2001, vol. 184, no. 2, pp. 319–325.

11. Haghuri-Gognet, A.-M. and Renard, J.-P., CMR Manganites: Physics, Thin Films, and Devices, *J. Phys. D: Appl. Phys.*, 2003, vol. 36, pp. R127–R150.
12. Belous, A.G., V'yunov, O.I., Yanchevskii, O.Z., et al. Oxidation State of Copper Ions in $La_{0.7}Sr_{0.3}Mn_{1-x}Cu_xO_{3\pm\delta}$ Ceramics and Their Magnetic Properties, *Neorg. Mater.*, 2006, vol. 42, no. 3, pp. 332–339 [*Inorg. Mater.* (Engl. Transl.), vol. 42, no. 3, pp. 286–293].
13. Shannon, R.D. and Prewitt, C.T., Effective Ionic Radii in Oxides and Fluorides, *Acta Crystallogr., Sect. B: Struct. Crystallogr. Cryst. Chem.*, 1969, vol. 25, no. 5, pp. 925–946.
14. Sun, Y., Tong, W., Xu, X., and Zhang, Y., Tuning Colossal Magnetoresistance Response by Cr Substitution in $La_{0.67}Sr_{0.33}MnO_3$, *Appl. Phys. Lett.*, 2001, vol. 78, no. 5, pp. 643–645.
15. Sully, A.H. and Brandes, E.A., *Chromium*, New York: Plenum, 1967, 2nd ed. Translated under the title *Khrom*, Moscow: Metallurgiya, 1971, p. 360.
16. Urushibara, A., Moritomo, Y., Arima, T., et al., Insulator–Metal Transition and Giant Magnetoresistance in $La_{1-x}Sr_xMnO_3$, *Phys. Rev. B: Condens. Matter Mater. Phys.*, 1995, vol. 51, no. 20, pp. 14103–14109.
17. Akimoto, T., Maruyama, Y., Moritomo, Y., and Nakamura, A., Antiferromagnetic Metallic State in Doped Manganites, *Phys. Rev. B: Condens. Matter Mater. Phys.*, 1998, vol. 57, no. 10, pp. 5594–5597.
18. Ghosh, K., Ogale, S.B., Ramesh, R., et al., Transition Element Doping Effects in $La_{0.7}Ca_{0.3}MnO_3$, *Phys. Rev. B: Condens. Matter Mater. Phys.*, 2000, vol. 59, no. 1, pp. 533–537.
19. Gross, R., Aleff, L., Bucher, B., et al., Physics of Grain Boundaries in the Colossal Magnetoresistance Manganites, *J. Magn. Magn. Mater.*, 2000, vol. 211, nos. 1–3, pp. 150–159.
20. Prodan, E.A., Pavlyuchenko, M.M., and Prodan, S.A., *Zakonomernosti topokhimicheskikh reaktsii* (General Mechanisms of Topochemical Reactions), Minsk: Nauka i Tekhnika, 1976.
21. Li, X.W., Gupta, A., and Xiao, G., Low-Field Magnetoresistive Properties of Polycrystalline and Epitaxial Perovskite Manganite Films, *Appl. Phys. Lett.*, 1997, vol. 71, no. 8, pp. 1124–1126.